



HAL
open science

Robust DNNs for power allocation problems in cognitive relay networks

Yacine Benatia, Anne Savard, Romain Negrel, E Veronica Belmega

► **To cite this version:**

Yacine Benatia, Anne Savard, Romain Negrel, E Veronica Belmega. Robust DNNs for power allocation problems in cognitive relay networks. 2024. hal-04698185

HAL Id: hal-04698185

<https://hal.science/hal-04698185v1>

Preprint submitted on 15 Sep 2024

HAL is a multi-disciplinary open access archive for the deposit and dissemination of scientific research documents, whether they are published or not. The documents may come from teaching and research institutions in France or abroad, or from public or private research centers.

L'archive ouverte pluridisciplinaire **HAL**, est destinée au dépôt et à la diffusion de documents scientifiques de niveau recherche, publiés ou non, émanant des établissements d'enseignement et de recherche français ou étrangers, des laboratoires publics ou privés.

Robust DNNs for power allocation problems in cognitive relay networks

Yacine Benatia, Anne Savard, *Senior Member, IEEE*, Romain Negrel, and E. Veronica Belmega, *Senior Member, IEEE*

Abstract—In this paper, we investigate deep neural network (DNN)-based power allocation policies maximizing the opportunistic rate of a relay-aided cognitive radio network under a quality of service (QoS) constraint protecting the primary transmission. The full-duplex relay performs either Decode-and-Forward (DF) or Compress-and-Forward (CF) and assists the opportunistic communication. The considered primary QoS constraint is expressed in terms of the tolerated primary rate degradation compared to the case of no opportunistic interference. In order to cope with imperfect channel state information (CSI) especially regarding the links to/from the primary network, we propose a self-supervised learning approach that skillfully exploits both perfect and imperfect CSI knowledge within the training phase. Since none of the two relaying schemes is optimal in all system setups (e.g., relative position of the different transmitters, receiver and of the relay), we then propose a novel supervised DNN-based relaying scheme selection. Finally, we extend all these results by proposing a self-supervised DNN-based power allocation policy that is able to generalize over system parameters such as the individual power budget, and the allowed level of primary degradation. Our extensive numerical results on synthetic data demonstrate the effectiveness of our proposed deep learning approaches.

Index Terms—Unsupervised deep learning, self-supervised deep learning, full-duplex relaying, cognitive radio, imperfect CSI.

I. INTRODUCTION

The recent massive increase in the number of connected users and devices is challenging future communication networks in terms of throughput, energy and spectral efficiency, etc. [1]. Several promising technologies, such as: cognitive radio, full-duplexing, cooperative communications, and artificial intelligence, etc. each of them focusing on specific goals, need to be jointly exploited [2]–[4].

On the one hand, cognitive radio and full-duplexing are key technologies to enable next-generation communication networks by tackling the spectrum scarcity. First, cognitive radio allows for a more efficient use of the available spectrum by providing unlicensed users (also termed as opportunistic or secondary users) with the access to the licensed frequency bands (i.e., allocated to licensed users, also termed as primary

users) as long as the induced interference satisfies some established quality of service [5], [6]. Second, under full-duplex communication, users can transmit and receive data simultaneously on the same frequency band, doubling hence the spectral efficiency [7].

On the other hand, cooperative communications are able to increase the network capacity and throughput by exploiting signals received from other users within range [8], [9]. The easiest model of such a cooperative network is the well-known relay channel, where one node, called relay, is willing to help a source node to communicate with its associated destination [10], [11]. The relay can perform various operations and three main relaying schemes, termed Amplify-and-Forward (AF), Decode-and-Forward (DF) and Compress-and-Forward (CF), have been proposed in the literature [11]. Under AF, the relay simply amplifies its received signal up to a power constraint before sending it to the destination node. DF and CF follow from information theory: under DF, the relay decodes the source message before re-encoding it and sending it to the destination; whereas under CF, the relay sends a compressed version of its received signal to the destination.

More recently, artificial intelligence and, in particular, deep learning (DL) has been shown to have an immense potential as a leading technology to address various challenges in future wireless networks. Indeed, DL has proven to be effective in reducing or replacing manual network configuration and management, optimizing communication resources, and adjusting system settings [3], [12], [13]. Additionally, DL techniques have been applied to solve resource optimization problems, which can greatly benefit future generations of networks, as evidenced by recent studies [14], [15].

In this paper, we jointly combine the above mentioned technologies to improve both the spectral efficiency and network throughput by considering a relay-aided cognitive radio network, where the opportunistic transmission is assisted by a full-duplex relay performing either DF or CF. In order to protect the licensed user, the opportunistic user and relay are allowed to transmit as long as the primary Quality of Service (QoS) constraint, expressed in terms of maximum allowed penalty on the achievable primary rate, is satisfied. We further focus on the case of imperfect channel state information (CSI) similarly to our previous study [16] and investigate how to best choose between DF and CF while optimizing the power allocation policy. We further study the robustness of our DNN-based approaches in terms of generalization over the system parameters, such as the power budget, the maximum allowed primary rate degradation.

Y. Benatia and E. V. Belmega are with ETIS UMR 8051, CY Cergy Paris Université, ENSEA, CNRS, F-95000, Cergy, France. A. Savard and Y. Benatia are with IMT Nord Europe, Institut Mines Télécom, Centre for Digital Systems, F-59653 Villeneuve d'Ascq, France. A. Savard is also with Univ. Lille, CNRS, Centrale Lille, UPHF, UMR 8520 - IEMN, F-59000 Lille, France. Y. Benatia and E. V. Belmega and R. Negrel are with Université Gustave Eiffel, CNRS, LIGM, F-77454, Marne-la-Vallée, France. Emails: {yacine.ben-atia, anne.savard}@imt-nord-europe.fr, {yacine.ben-atia, romain.negrel, veronica.belmega}@esiee.fr.

A. Existing works

Because of the operations performed at the relay, the resulting power allocation problems in such a relay-aided cognitive network are non-convex ones, which are hard to solve analytically [16]–[18]. Instead, iterative methods have been proposed to maximize the sum-rate of multi-users networks, such as weighted minimum mean square error [19] in MIMO interfering broadcast channels or iterative water-filling [20] in cognitive radio network exploiting Orthogonal Frequency Division Multiplexing (OFDM). However, these methods may converge very slowly to only a local extremum in the aforementioned non-convex settings and may not be able to handle imperfect CSI, especially when the number of users is large [21], [22].

To overcome these issues, we exploit deep neural networks (DNN), which were shown to provide good approximations of the optimal solutions in complex and non-convex optimization problems with low computational complexity compared to exhaustive search [14], [22]–[31]. Recently, DNN-based resource allocation policies have been widely applied in multi-user networks when either maximizing the achievable sum rate [14], the spectral efficiency [21], [22], [24] or the energy efficiency [23], [32]. The considered networks rely either on D2D communications constrained by both a total power budget and some QoS constraints [21], [22], on non-orthogonal multiple access under QoS and total power budget [23], on massive MIMO under total power budget constraint [24], on wireless-powered network under a power budget [32] or on multi-user interference channel [14].

Moreover, DNN-based resource allocation policies have also been proposed in cognitive radio networks to maximize the spectral efficiency under power budget and QoS requirements protecting the primary users [15], [33], [34], or to minimize the consumed power ensuring that a predefined signal to noise interference ratio is met for both the primary and secondary users [35].

Regarding relay selection and relaying scheme selection, different approaches can be found in the literature. On the one hand, many works can be found regarding relay selection, where the best relay node among multiple relay candidates [36], [37] has to be chosen. Usually, the selection is performed such that the relay maximizing the achievable rate (or the signal to noise ratio) [36] or the spectral efficiency [37] is chosen. This search task can be performed using DNN [37]–[39]. On the other hand, relaying scheme selection focuses on choosing among different relaying schemes, the one yielding the best performance. For example, in [40], [41] both AF and DF relaying schemes were considered, where the selection criterion was to maximize the signal to noise ratio in [40], whereas the authors of [41] considered an outage-based and symbol error rate-based method.

Regarding the robustness to channel state information (CSI) imperfections, a DNN-based autoencoder enhancing the channel estimation quality has been proposed in [42]. The latter was then used as the input of a second DNN to maximize the achievable sum-rate of cognitive radio networks. In [22], a power allocation policy maximizing the average spectral

efficiency of the D2D user, while maintaining the QoS of the cellular user equipment to an allowable level under imperfect CSI was proposed for underlay D2D communications. The effect of imperfect CSI was tackled via DNN, such that the proposed power allocation policy was robust to channel estimation errors.

The closest works are our two previous studies [16], [18]. To the best of our knowledge, our previous study [18] was the first one to exploit unsupervised DNN to solve resource allocation in cooperative cognitive networks. In the latter, we assumed that perfect CSI was available throughout the network. Since perfect CSI especially for the links related to the primary network is difficult to obtain, we then relaxed this assumption and extended our proposed approach to the case of imperfect CSI in [16], in which we proposed a robust training procedure.

In this paper, we extend our previous studies by first comparing the two relaying schemes in terms of opportunistic achievable rates and primary protection as a function of the node positions, leading to the problem of relay scheme selection; and then propose a new self-supervised DNN able to generalize over several system parameters (power budget of the secondary network, requirement protection of the primary transmission).

B. Main contributions

Specifically, our main contributions can be summarized as follows.

- We first propose a self-supervised DNN-based power allocation policy maximizing the secondary instantaneous rate assuming either DF or CF relaying, imperfect CSI, and under a QoS constraint protecting the primary transmission as well as individual transmit power constraints. Unlike classical optimization approaches that are quite sensitive to imperfect CSI, we show that our DNN-based approach can be efficiently rendered robust via self-supervised learning based on training data that contains coupled samples of perfect and imperfect channels. The obtained secondary rates as well as primary degradation under each of the relaying schemes are then investigated as functions of the relay position, leading to representative regions where one of the two relaying schemes is more suited.
- Motivated by the above, we then investigate the relaying scheme selection issue and propose two strategies. Our first strategy exploits our aforementioned self-supervised based scheme under DF and CF. The second one involves an extra DNN alongside a supervised learning approach. The two schemes are compared both in terms of secondary rates, as well as in terms of primary degradation. By tuning a threshold parameter within the extra DNN approach, we show that the primary transmission can be better protected at the cost of secondary rate.
- Finally, we generalize all the above to the case where the system parameters, i.e., power budgets and primary degradation parameter are not fixed but can vary within a given range. This demonstrates the flexibility and generalization capability of our proposed approaches.

The rest of the paper is organized as follows: Section II presents system model under study. In Section III, we introduce our self-supervised DNN-based power allocation under

both CF and DF assuming imperfect CSI, alongside with numerical performance of each of the relaying schemes. We then propose several relaying scheme selection strategies and compare one to each other in Section IV. In Section V, we present our proposed generalized self-supervised DNN-based power allocation policy that is able to adapt to various power budgets and levels of allowed primary degradation. Finally, Section VI concludes the paper.

II. SYSTEM MODEL AND PROBLEM FORMULATION

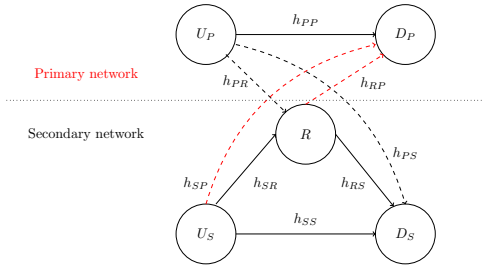


Figure 1: Cognitive relay-aided network under study

The cognitive relay-aided network under study is illustrated in Figure 1 and consists of a primary transmitter U_P and its associated destination D_P , as well as a secondary transmitter U_S and its associated destination D_S , the latter being assisted by a full-duplex relay node, as in our previous studies [16]–[18]. Let X_P , X_S and X_R , of average power P_P , P_S and P_R , denote the messages sent by U_P , U_S and the relay respectively. Further, let Z_R and Z_i , $i \in \{S, P\}$ denote the additive white Gaussian noise (AWGN), of variance N_R and N_i , at the relay and at destination D_i respectively. As in [16]–[18], [43], we consider a full-duplex operating relay that is perfectly cancels out any self interference. The received signals at the relay, primary and secondary destination are thus expressed as

$$Y_R = h_{PR}X_P + h_{SR}X_S + Z_R \quad (1)$$

$$Y_i = h_{Ri}X_R + h_{ii}X_i + h_{ji}X_j + Z_j, \quad (2)$$

where $i, j \in \{P, S\}$, $i \neq j$.

Throughout this paper, and without loss of generality, we assume that the additive noise terms are of unit variance, $N_R = N_S = N_P = 1$; or equivalently we consider channel gains normalized by the received noise variance and given as $g_{ij} = \frac{h_{ij}^2}{N_j}$, $\forall i, j \in \{S, P, R\}$. To simplify the presentation, we let $\mathbf{h} = \{\sqrt{g_{ij}}, \forall i, j\}$ denote the collection of all normalized channels in the network. Furthermore, the relay only helps the opportunistic transmission, as such the message from the relay and from the secondary user are treated as additional noise at the primary destination when retrieving its own information X_P . In the same manner, the message from the primary user is considered as additional noise at both the relay and the secondary destination when recovering X_S . Hence, we can consider equivalent correlated additive Gaussian noises at the relay and secondary destination defined as $\tilde{Z}_R = h_{PR}X_P + Z_R$ and $\tilde{Z}_S = h_{PS}X_P + Z_S$, of variance $\tilde{N}_R = g_{PR}P_P + 1$ and $\tilde{N}_S = g_{PS}P_P + 1$ respectively; where the correlation coefficient is given as $\rho_Z = \frac{\sqrt{g_{PR}g_{PS}P_P}}{\sqrt{\tilde{N}_R\tilde{N}_S}}$.

Let R_i , $i \in \{P, S\}$ denote the achievable rate of the primary and secondary user respectively. Let \overline{R}_P denote the achievable primary rate in the absence of the opportunistic network, which is expressed as $\overline{R}_P = 1/2 \log_2(1 + g_{PP}P_P)$. As in our previous studies [16]–[18], the opportunistic network is allowed to communicate over the licensed bands provided that the primary achievable rate is not degraded below a fraction $(1 - \tau)$ of its achievable rate in the absence of the secondary network: the considered QoS protecting the primary user is hence expressed as $R_P \geq (1 - \tau)\overline{R}_P$, $\tau \in [0, 1]$.

a) *Problem under study:* In this paper, our objective is three-fold. First, we maximize the opportunistic achievable rate under both CF and DF subject to maximum power constraints at the relay and secondary user respectively, and to a QoS constraint protecting the primary transmission. We consider that all channel links related to the primary network are impaired by estimation errors. Our optimal resource allocation policy is obtained by a self-supervised DNN coupled with a robust training technique. Second, we wish to select the best relaying scheme among CF and DF, when the goal is to degrade the least the primary transmission. We proposed two selection approaches, one exploiting only the aforementioned robust self-supervised DNN for both CF and DF; and one exploiting an additional DNN. Third, we derive new robust self-supervised DNNs able to generalize over several system parameters such as the total power budgets \overline{P}_S , \overline{P}_R or the maximum allowed primary degradation.

b) *Imperfect CSI:* As in our previous study [16], we assume here that the channel gains are impaired by estimation errors. The channel errors are modeled as additive Gaussian noise as in [42], [44] and only affect the links from the secondary network to the primary one, as we assume that perfect CSI can be obtained by the help of pilot symbols within the secondary network. Since the secondary user transmits in an opportunistic manner, it is unlikely for the primary network to feedback any channel estimation to the secondary user and relay. Hence, $\hat{h}_{ij} = h_{ij} + \varepsilon_{ij}$, $\varepsilon_{ij} \sim \mathcal{N}(0, \sigma_{\varepsilon_{ij}}^2)$, $\forall (i, j) \in \{(P, P), (S, P), (R, P), (P, R), \text{ and } (P, S)\}$ and the normalized estimated channel gains are given as $\hat{g}_{ij} = (\hat{h}_{ij})^2/N_j$. In the above, the estimation error variance is assumed to be of the form $\sigma_{\varepsilon_{ij}}^2 = \text{Var}[h_{ij}]/\text{SNR}$, where $\text{Var}[h_{ij}]$ denotes the variance of the true channels h_{ij} and $\text{SNR} \in [-10, 20]$ dB represents the signal-to-noise ratio (SNR) of the estimator. The normalized channel gains within the secondary network are on the other hand perfectly known and given as $\hat{g}_{ij} = (\hat{h}_{ij})^2/N_j = \hat{h}_{ij}/N_j = h_{ij}/N_j$, $\forall (i, j) \in \{(S, S), (S, R), \text{ and } (R, S)\}$. We henceforth let $\hat{\mathbf{h}}$ denote the vector collecting all the estimated channel links.

Notations: To simplify the presentation, the following notation will be used. $A = \frac{g_{PP}P_P}{(1+g_{PP}P_P)^{1-\tau-1}} - 1$, $[x]^+ = \max\{0, x\}$ and $C(x) = \frac{1}{2} \log_2(1+x)$ denotes the capacity of the point-to-point AWGN channel. Let K_1, K_2 denote

$$K_1 = g_{SR}\tilde{N}_S + g_{SS}\tilde{N}_R - 2\rho_Z \sqrt{g_{SR}g_{SS}\tilde{N}_S\tilde{N}_R},$$

$$K_2 = (1 - \rho_Z^2)\tilde{N}_R\tilde{N}_S.$$

III. SELF-SUPERVISED DNN BASED POWER ALLOCATION POLICY UNDER IMPERFECT CSI

We first start by presenting the optimization problem under both CF and DF, as studied in [16], and then present our proposed DNN solution as well as some numerical results and comparison between the two relaying schemes.

Under both CF and DF, the considered optimization problem writes as

$$\begin{aligned} (\mathbf{OP}) \quad & \max_{P_R, P_S} R_S(\mathbf{h}, P_S, P_R) \\ \text{s.t.} \quad & R_P(\mathbf{h}, P_S, P_R) \geq (1 - \tau)\overline{R_P}, \\ & 0 \leq P_S \leq \overline{P_S}, \quad 0 \leq P_R \leq \overline{P_R}, \end{aligned}$$

where the secondary and primary achievable rates $R_S(\mathbf{h}, P_S, P_R)$ and $R_P(\mathbf{h}, P_S, P_R)$ depend on the relaying scheme.

We focus next on the specific optimization problems when replacing the achievable rate regions obtained under CF and DF of [17] into the above optimization problem (**OP**).

A. Compress-and-Forward (CF)

Under CF, exploiting the achievable rate region of [17] leads to the following optimization problem

$$\begin{aligned} (\mathbf{OCF}) \quad & \max_{P_R, P_S} R_S(\mathbf{h}, P_S, P_R) \\ \text{s.t.} \quad & Q(\mathbf{h}, P_S, P_R) \leq A, \quad (\text{QoS}) \\ & 0 \leq P_S \leq \overline{P_S}, \quad 0 \leq P_R \leq \overline{P_R}, \text{ with } (\text{TP}) \end{aligned}$$

$$R_S(\mathbf{h}, P_S, P_R) = C \left(\frac{K_1 g_{RS} P_S P_R + g_{SS} P_S (K_1 P_S + K_2)}{K_2 g_{RS} P_R + \tilde{N}_S (K_1 P_S + K_2)} \right)$$

$$Q(\mathbf{h}, P_S, P_R) = g_{SP} P_S + g_{RP} P_R.$$

Although non-convex, this optimization problem can be solved in closed-form under perfect CSI, as shown in our previous work [16]. Nonetheless, our closed-form solution highly relies on the perfect CSI knowledge, which can be difficult to obtain, especially for the channel links related to the primary network. As such, we proposed in [16] to exploit a self-supervised DNN-based resource allocation coupled with a robust training to cope with imperfect CSI, as detailed in Section III-C, instead of taking into the imperfect CSI within the problem formulation, which generally does not lead to closed-form solutions [21], [45].

B. Decode-and-Forward (DF)

Under DF, exploiting the achievable rate region of [17] leads to the following optimization problem

$$\begin{aligned} (\mathbf{ODF}) \quad & \max_{P_R, P_S, \alpha} R_S(\mathbf{h}, \alpha, P_S, P_R) \\ \text{s.t.} \quad & Q(\mathbf{h}, \alpha, P_S, P_R) \leq A, \quad (\text{QoS}') \\ & 0 \leq P_S \leq \overline{P_S}, \quad 0 \leq P_R \leq \overline{P_R}, \quad (\text{TP}) \\ & 0 \leq \alpha \leq 1, \text{ with } (\text{ADF}) \end{aligned}$$

$$\begin{aligned} R_S(\mathbf{h}, \alpha, P_S, P_R) &= C(\min\{f_R(\mathbf{h}, \alpha, P_S, P_R), f_S(\mathbf{h}, \alpha, P_S, P_R)\}) \\ Q(\mathbf{h}, \alpha, P_S, P_R) &= g_{SP} P_S + g_{RP} P_R + 2\alpha \sqrt{g_{SP} g_{RP} P_S P_R}, \\ f_R(\mathbf{h}, \alpha, P_S, P_R) &= \frac{g_{SR}(1 - \alpha^2) P_S}{\tilde{N}_R}, \\ f_S(\mathbf{h}, \alpha, P_S, P_R) &= \frac{g_{SS} P_S + g_{RS} P_R + 2\alpha \sqrt{g_{RS} g_{SS} P_S P_R}}{\tilde{N}_S}, \end{aligned}$$

where the additional variable $\alpha \in [0, 1]$ trades-off between sending a new codeword and repeating the previous one under the information-theoretic superposition coding.

Compared to CF relaying, because of the more complex expressions (including square root terms) of the non-convex objective function coupled with a non-convex QoS constraint (as opposed to an affine one for CF) involving an additional variable α under DF, obtaining the solution of the optimization problem (**ODF**) in closed form is very challenging, if at all possible, even under perfect CSI. Hence, in the imperfect CSI case under study, we propose to turn to self-supervised learning-based approaches [16] as detailed later on in Section III-C.

Below, we present our self-supervised DNN approach able to cope with imperfect CSI under both CF and DF. Henceforth, we denote the primary and secondary rate by $R_P(\mathbf{h}, \alpha, P_S, P_R)$ and $R_S(\mathbf{h}, \alpha, P_S, P_R)$ respectively, to include both DF and CF relaying, where under CF the extra DF-parameter α following from superposition coding is set to $\alpha = 0$.

C. Our DNN-based solution

Our self-supervised approach exploits a customized loss function coupled with a robust training procedure based on a dataset composed of coupled perfect and imperfect channel estimations pairs $(\hat{\mathbf{h}}_\ell, \mathbf{h}_\ell)_\ell$. Nevertheless, only the imperfect channel estimations are given as inputs to the DNN during both the training and the test phases; the perfect channel estimations are only fed to the loss function during training.

The key ingredient of our proposed self-supervised DNN-based solution is the customized loss function that the DNN is trained to minimize, coupled with the training data (composed of labeled pairs of perfect-imperfect channel gains) described above. Since the QoS constraint is more a requirement than a physical hard constraint, we propose to relax it and incorporate it in the loss function via an additional hyperparameter λ as follows

$$\begin{aligned} \mathcal{L}(\mathbf{h}_\ell, \hat{\mathbf{h}}_\ell) &= \sum_{\ell=1}^N \left(-R_S \left(\mathbf{h}_\ell, \hat{\alpha}(\hat{\mathbf{h}}_\ell), \hat{P}_S(\hat{\mathbf{h}}_\ell), \hat{P}_R(\hat{\mathbf{h}}_\ell) \right) \right. \\ &\quad \left. + \lambda \left[(1 - \tau)\overline{R_P}(\mathbf{h}_\ell) - R_P \left(\mathbf{h}_\ell, \hat{\alpha}(\hat{\mathbf{h}}_\ell), \hat{P}_S(\hat{\mathbf{h}}_\ell), \hat{P}_R(\hat{\mathbf{h}}_\ell) \right) \right]^+ \right), \end{aligned}$$

where N denotes the number of available channel samples that are perfectly estimated in the training dataset. The additional hyperparameter λ trade-offs between a secondary rate-driven objective and a primary QoS-driven objective. Hence, this parameter should be carefully tuned, as detailed in [18]. In the rest of this paper, we choose $\lambda = 10^{0.5}$ due to its good compromise between the achievable secondary rate and the primary QoS degradation.

Under imperfect CSI, another performance metric to be considered is the outage probability defined as:

$$P_{out} = \Pr \left[R_S \left(\mathbf{h}, \hat{\alpha}(\hat{\mathbf{h}}_\ell), \hat{P}_S(\hat{\mathbf{h}}_\ell), \hat{P}_R(\hat{\mathbf{h}}_\ell) \right) < r \right],$$

where r denotes the fixed transmit rate and the probability is taken with respect to the randomness in the system channels \mathbf{h} . In our study, we propose a simplified approach compared to minimizing the outage probability, where the training dataset contains perfect CSI \mathbf{h} , alongside with estimated channels $\hat{\mathbf{h}}$ impaired by estimation errors, and our DNN aims at maximizing the instantaneous rates $R_S \left(\mathbf{h}_\ell, \hat{\alpha}(\hat{\mathbf{h}}_\ell), \hat{P}_S(\hat{\mathbf{h}}_\ell), \hat{P}_R(\hat{\mathbf{h}}_\ell) \right)$, a term similar to that used in the context of minimizing outage probability. Therefore, we can conjecture that our approach should also perform well in terms of outage probability.

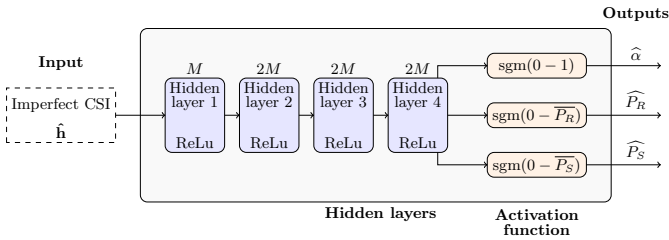


Figure 2: Proposed DNN architecture, where \hat{x} denotes the estimated or the predicted quantity x .

Based on extensive numerical simulations, we have chosen the following architecture for our proposed self-supervised DNN: four fully connected hidden layers of $M - 2M - 2M - 2M$ neurons, with $M = 128$, followed by a rectified linear unit (ReLU) activation function, as illustrated in Figure 2. The final layer is followed by sigmoid activation functions to ensure that the outputs, i.e., the predicted values of the powers P_R , P_S and the predicted value of α under DF satisfy the box-type constraints of (OP). Note that our proposed self-supervised DNN is specifically training for either CF or DF and for fixed values of the network parameters \overline{P}_R , \overline{P}_S and τ . The later will be relaxed in Section V.

D. Numerical results

In this section, we investigate the robustness of our proposed self-supervised DNN-based power optimization under imperfect CSI.

a) *Dataset*: As in our previous studies [16], [18], our training dataset contains 10^6 samples of both perfect and imperfect channel estimations $\{\hat{\mathbf{h}}_\ell, \mathbf{h}_\ell\}_\ell$. The validation dataset contains 2×10^5 samples of both perfect and imperfect channel estimations $\{\hat{\mathbf{h}}_\ell, \mathbf{h}_\ell\}_\ell$, while the test dataset contains 2×10^5 samples of imperfect channel estimations $\{\hat{\mathbf{h}}_\ell\}_\ell$. These datasets are disjoint.

Here, we assume that the channel gains follow a common fading and pathloss model as $h_{ij} \sim \frac{\mathcal{N}(0, \sigma_g^2)}{\sqrt{1 + d_{ij}^\gamma}}$, where d_{ij} is distance between nodes i and j as in our previous studies [16], [18]. The pathloss is set to $\gamma = 3$, the channel gain standard deviation to $\sigma = 7$ and other network parameters are set to $\tau = 25\%$ and $P_P = \overline{P}_S = \overline{P}_R = 10$ W. We further assume

that all node's positions are generated uniformly within a 10 m square cell unless otherwise specified.

b) *DNN training*: As in [16], we assume that in the training phase, we have access to pairs of both perfect and imperfect channel estimations $\{\hat{\mathbf{h}}_\ell, \mathbf{h}_\ell\}_\ell$, where the imperfect ones are obtained by adding Gaussian noise to the initial ones. The perfect channel estimations are fed to our loss function \mathcal{L} , whereas the imperfect channel estimations are given as the input of our self-supervised DNN and the training process is restarted for each value of the considered channel estimated SNR. To avoid overfitting effects, an early-stopping method is adopted for both DF and CF with a patience parameter of 20 epochs.

c) *Benchmarks and performance metrics*: In the following, we propose to compare our self-supervised DNN-based predictions under imperfect CSI to the optimal power allocation policies under perfect CSI. The latter are obtained either in closed form under CF [16] or by brute force (exhaustive/grid search) under DF. Thanks to its implementation simplicity, we chose to use brute force to compensate for the lack of closed-form expression under DF. We consider three metrics to validate the performance of our self-supervised DNN-based method under imperfect CSI: the relative gap G , the empirical outage Outage and the average primary rate degradation Δ_{out} , defined below.

The *relative gap* G assesses the gap between the predicted rate $\hat{R}_{S,\ell} = R_S \left(\mathbf{h}_\ell, \hat{\alpha}(\hat{\mathbf{h}}_\ell), \hat{P}_S(\hat{\mathbf{h}}_\ell), \hat{P}_R(\hat{\mathbf{h}}_\ell) \right)$, achieved by either the self-supervised DNN or the benchmark under imperfect CSI, and the ideal optimal rate $R_{S,\ell}^* = R_S \left(\mathbf{h}_\ell, \hat{\alpha}(\mathbf{h}_\ell), \hat{P}_S(\mathbf{h}_\ell), \hat{P}_R(\mathbf{h}_\ell) \right)$ obtained with the benchmark under perfect CSI, for each sample in the dataset:

$$G = \frac{\frac{1}{N} \sum_{\ell=1}^N \hat{R}_{S,\ell} - R_{S,\ell}^*}{\frac{1}{N} \sum_{\ell=1}^N R_{S,\ell}^*}. \quad (3)$$

The two other metrics rely on the degradation of the primary rate defined as

$$\Delta_\ell = 1 - \frac{R_P \left(\mathbf{h}_\ell, \hat{\alpha}(\hat{\mathbf{h}}_\ell), \hat{P}_S(\hat{\mathbf{h}}_\ell), \hat{P}_R(\hat{\mathbf{h}}_\ell) \right)}{\overline{R}_P(\mathbf{h}_\ell)}, \quad (4)$$

where $R_P \left(\mathbf{h}_\ell, \hat{\alpha}(\hat{\mathbf{h}}_\ell), \hat{P}_S(\hat{\mathbf{h}}_\ell), \hat{P}_R(\hat{\mathbf{h}}_\ell) \right)$ corresponds to the primary rate achieved either by our proposed self-supervised DNN or the benchmark under imperfect CSI and $\overline{R}_P(\mathbf{h}_\ell)$ is the primary achievable rate obtained under perfect CSI. The *empirical outage* is defined as the proportion of samples in the dataset for which the primary QoS is not satisfied, whereas the *average primary rate degradation* computes the primary rate degradation when in outage:

$$\text{Outage} = \frac{1}{N} \sum_{\ell=1}^N \mathbb{1}[\Delta_\ell > \tau], \quad \Delta_{out} = \frac{\sum_{\ell=1}^N (\mathbb{1}[\Delta_\ell > \tau] \times \Delta_\ell)}{\sum_{\ell=1}^N \mathbb{1}[\Delta_\ell > \tau]},$$

where $\mathbb{1}$ is the indicator function.

d) *Numerical simulations*: Figure 3 and Figure 4 present the robustness to imperfect CSI in terms of relative gap, outage and average primary rate degradation as a function of the SNR of the channel estimation under CF and DF respectively. Under

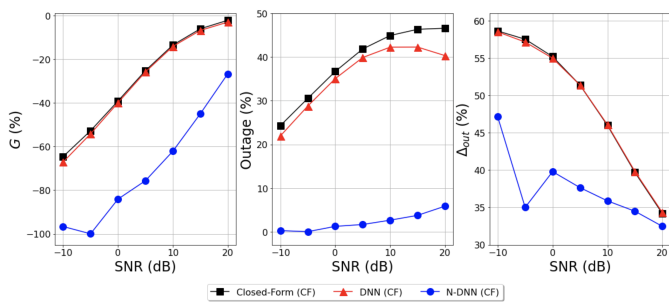


Figure 3: Impact of imperfect CSI on our proposed solutions for CF relaying over the test set.

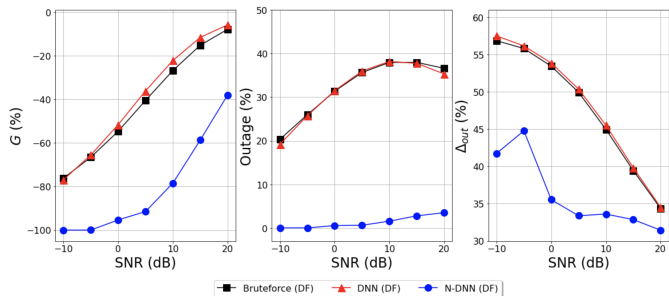


Figure 4: Impact of imperfect CSI on our proposed solutions for DF relaying over the test set.

both CF and DF, we compare the performance achieved by the benchmark under imperfect CSI (either closed-form expression under CF or brute-force under DF), the one achieved by our unsupervised DNN trained only with perfect CSI labeled as “DNN”, and the one achieved with our new proposed robust training labeled as “N-DNN”, i.e., when both perfect and imperfect CSI are used in the training phase. First, note that although designed initially for DF, our proposed unsupervised DNN is able to generalize to CF relaying as well with almost no architecture change beside removing one of the predicted output, as can be seen from the almost zero gap between the performance achieved by the benchmark and by the unsupervised DNN.

Second, for all relaying schemes, both the benchmark and the unsupervised DNN trained with only perfect CSI harm the primary communication in almost 20 – 50% of cases with an average primary rate degradation when in outage between 35 and 65%, highly above the defined threshold $\tau = 25\%$. On the contrary, our self-supervised DNN with robust training achieves lower secondary rate compared to the benchmark or to the unsupervised DNN trained only with perfect CSI (loss in terms of relative gap of the order of 20 – 40%) but satisfies almost always the QoS constraint with an outage of only 5%, which is crucial in cognitive radio setups. Furthermore, when in outage, the primary rate degradation is kept below 45%. One can also note that the outage under CF is less than that under DF, which is to be expected since the optimization problem under DF is more difficult to solve due to the non-convex objective function and QoS constraint.

Once our proposed robust training has been validated, we can focus on the comparison of the two relaying schemes

as a function of the nodes spatial positions within the considered square cell. More specifically, we now assume that the positions of the primary and secondary user/destination pairs are fixed and given as $U_S(3.2, 3)$, $D_S(6.5, 1)$, $U_P(2, 7)$, $D_P(6.5, 8.5)$, such that the direct links are stronger than the interfering ones; whereas the relay can be placed anywhere within the cell.

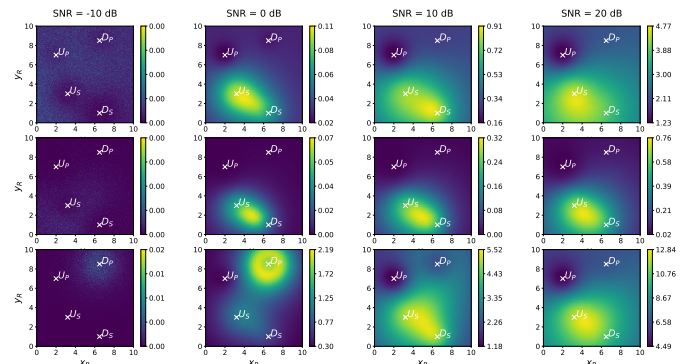


Figure 5: Impact of the relay position for DF relaying. Top plots: average total power (W); middle: average secondary rate (bpsu); bottom: average primary rate degradation (%).

Figure 5 depicts the average power transmitted by the secondary network, the average secondary rate as well as the average primary rate degradation for four different channel estimation SNRs under DF relaying. Each simulation result has been averaged over 10^4 random channel realizations, not included in the test set. The channel gains for these simulations are generated in the same manner as described in Section III-D. Under poor channel estimation, $\text{SNR} \in \{-10, 0\}$ dB, the secondary network barely transmits at all, leading to almost no primary rate degradation and almost zero secondary rate. As the quality of the CSI increases, i.e. $\text{SNR} \in \{10, 20\}$ dB, one can note that DF performs well in terms of secondary rate when the relay is close to the secondary user, as for the standard relay channel. Furthermore, in all cases, one can see that the average primary rate degradation stays below the fixed threshold value of $\tau = 25\%$. At last, when $\text{SNR} = 0$ dB, we can observe that although the power of the secondary communication is very small when the relay is in close proximity of the primary receiver, such a configuration has a marginally degrading impact to the primary communication. This is equivalent to the case of $\text{SNR} = 10$ dB, where the primary degradation is about 2% when the relay is close to the primary receiver. To understand this counter-intuitive behavior, we study in the top plots of Figure 6 the maximum primary rate degradation as a function of the relay position for $\text{SNR} = 0$ dB and $\text{SNR} = 10$ dB, and we can note the presence of a noise, corresponding to outliers where the primary rate degradation reaches 100%, when computing this maximum. In order to mitigate the influence of this added noise, we apply a median filter [46]. Interestingly, we observe that as we increase the radius of the disk-shaped mask used for filtering, the noise progressively decreases, as shown in the bottom plots of Figure 6 (maximum of primary degradation with median filter when disk radius is equal to 3), and that

the maximum of degradation is around the primary receiver.

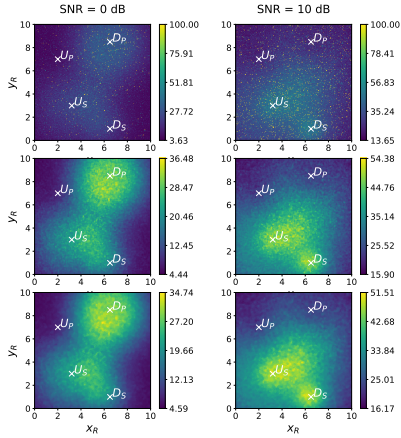


Figure 6: Impact of the relay position for DF relaying (maximum of primary degradation (%)). Top plots: maximum of primary degradation without median filter; middle: maximum of primary degradation with median filter (disk radius = 2); bottom: maximum of primary degradation with median filter (disk radius = 3).

Regarding CF relaying, we conduct similar numerical experiments.

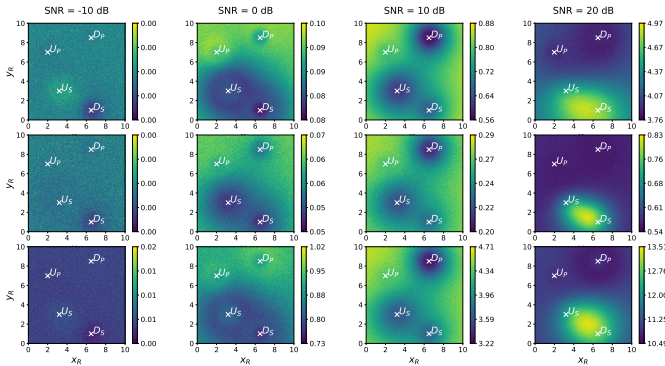


Figure 7: Impact of the relay position for CF relaying. Top plots: average total power (W); middle: average secondary rate (bps); bottom: average primary rate degradation (%).

The results showing the average power transmitted by the secondary network, the average secondary rate, and the average primary rate degradation for four different channel estimation SNRs are presented in Figure 7. Similar to DF, in the case of poor channel estimation $\text{SNR} \in \{-10, 0\}$ dB, the secondary network exhibits minimal transmission, resulting in no primary rate degradation and nearly zero secondary rate. As the quality of the CSI improves ($\text{SNR} = 20$ dB), we can observe that CF performs best when the relay is close to the secondary destination. Furthermore, in all cases, the average degradation of the primary rate remains below the predetermined threshold value of $\tau = 25\%$. These observations hold true across all the simulations, each of which averages results over 10^4 channel realizations, as for DF relaying.

In Figure 7, it can be inferred that when $\text{SNR} \in \{-10, 0, 10\}$ dB, indicating a significant amount of estimation error, the utilization of the relay decreases. To investigate

these cases, further exploration of the self-supervised DNN performance and the hyperparameter λ are necessary in order to improve the relay's effectiveness under such conditions. We opt to explore the impact of the hyperparameter λ variation to see whether a lower λ value results in increased utilization of the relay.

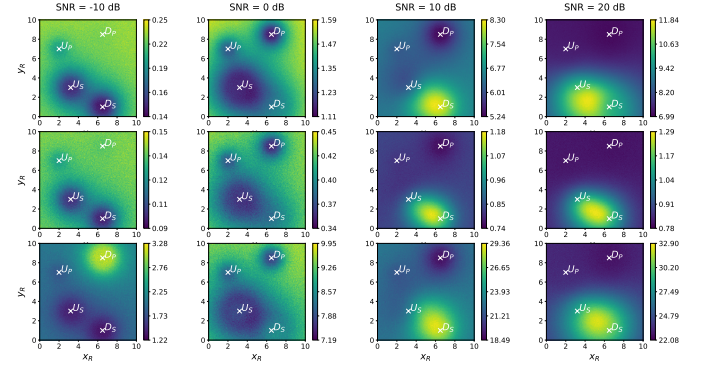


Figure 8: Impact of the relay position for CF relaying ($\lambda = 10^{-0.5}$). Top plots: average total power (W); middle: average secondary rate (bps); bottom: average primary rate degradation (%).

When we modify λ from $10^{0.5}$ to $10^{-0.5}$, as shown in Figure 8, its impact becomes evident. We observe that as the value of λ decreases, the relay utilization increases, leading consequently to an improved secondary rate, as expected. However, it is noteworthy that this enhancement in throughput comes at the expense of significant degradation in the primary communication, reaching up to 32%. This degradation exceeded our predefined threshold of 25%, indicating a notable decrease in the primary communication's overall quality.

IV. RELAYING SCHEME SELECTION

As discussed in the previous section, none of the two relaying schemes performs best for all network parameters and configurations. In this section, we investigate the problem of selecting the relaying scheme and we propose two different approaches to choose among CF and DF. In our cognitive radio setting, we focus the relay scheme selection on protecting the primary network, which of course may lead to a cost in terms of secondary achievable rate.

A. First relaying scheme selection

Usually, relaying scheme selection consists in choosing the relaying scheme achieving the largest SNR [36], [40]. Such a criterion is well-suited for many communication models but not for cognitive radio networks where one should also protect the primary transmission.

To simplify the presentation, let us denote by R_S^{CF} , R_S^{DF} the secondary rate achieved by CF and DF respectively. We further let Δ_ℓ^{CF} and Δ_ℓ^{DF} denote the degradation of the primary achievable rate caused by the opportunistic transmission under CF and DF.

In order to choose between CF and DF, we propose the following scheme. First we compare the two degradations of the primary rate Δ_ℓ^{CF} and Δ_ℓ^{DF} . If both relaying scheme meet

the QoS constraint and are somewhat equivalent in terms of primary degradation, i.e. $\Delta_\ell^{CF}, \Delta_\ell^{DF} \leq \tau$, then we choose the relaying scheme yielding the largest secondary rate. If only one of the relaying scheme meets the QoS constraint, then we choose this scheme. At last, if neither relaying scheme meets the QoS constraint, we then choose the one inflicting the least primary rate degradation. Hence, we put more emphasis on meeting the primary QoS constraint, at the cost of the secondary rate.

We will exploit this first relaying scheme selection both as a benchmark and also to build ground-truth data for our second relaying scheme selection method, described in the next subsection, which exploits the two DNNs designed for CF and DF as well as an additional one to decide between CF and DF.

a) Benchmark: When used as benchmark to compare the performance of our two proposed methods, the achievable rates and the primary QoS degradation are computed using the predicted powers of DF and CF with imperfect CSI as the DNN inputs as well as imperfect CSI within the rate computations. Indeed, when predicting the optimal power allocations and also when deciding between DF and CF, the secondary user has access only to an imperfect CSI.

b) New dataset generation: To build the new data used for our second relaying scheme selection method, we make use of the perfect CSI to compute the achievable rates and the primary degradation but given the predicted powers obtained with imperfect CSI as the DNN inputs. Indeed, we assume that for training purposes, we have access to high-quality or perfect CSI estimations similarly to the training of the DNNs predicting the power allocations in Section III.

More precisely, for the ℓ -th entry of our new dataset, we first compute the estimated powers $\hat{P}_R(\hat{\mathbf{h}}_\ell), \hat{P}_S(\hat{\mathbf{h}}_\ell)$ under DF and CF obtained as outputs of the aforementioned DNNs with the imperfect channel estimations as inputs. Once the estimated powers are obtained, we compute the achievable rates and the primary rate degradations, under both CF and DF, by using the true channel gains (perfect estimation), i.e. $R_S(\mathbf{h}_\ell, \hat{\alpha}(\hat{\mathbf{h}}_\ell), \hat{P}_S(\hat{\mathbf{h}}_\ell), \hat{P}_R(\hat{\mathbf{h}}_\ell))$ and Δ_ℓ . Finally, we use the first relaying scheme selection method above to select between CF and DF for all CSI samples in our dataset. As such, the ℓ -th entry of our dataset contains: the perfect and imperfect channel estimations, the associated optimal powers obtained via the self-supervised DNN described in Section III-C as well as the corresponding selected relaying scheme.

Note that while we can exploit perfect CSI to build a dataset for training purposes, perfect CSI cannot be used to select the relaying scheme in the running phase. Indeed, making use of this knowledge would imply first to transmit with DF and then CF, then to compute the true achievable rates at the receiver and feedback them to the transmitter, and finally to select the best relaying scheme for the next transmission, which is not realistic.

B. Second relaying scheme selection

In this section, we introduce a novel supervised DNN-based relaying scheme selection, where a DNN takes as inputs the

imperfect channel estimations as well as the corresponding optimal power allocations under both DF and CF, computed by our previously presented self-supervised DNN methods of Section IV-B, and outputs the best relaying scheme.

Our intuition is that, whereas the previously presented approach only exploits two DNNs specifically trained for either DF or CF, an additional DNN could improve the relay scheme selection by learning some correlation between the imperfect channel gains and the best relaying scheme exploiting both imperfect CSI to predict the transmissions parameters and perfect CSI to select among CF and DF (the latter being available during its training).

We hence consider a binary classification problem, for which the binary cross-entropy, given below, is usually used as loss function [47], [48]:

$$\mathcal{L} = -\frac{1}{L} \sum_{i=1}^L y_i \log \hat{y}_i + (1 - y_i) \log(1 - \hat{y}_i), \quad (5)$$

where L is the number of available training data samples; $y_i \in \{0, 1\}$ corresponds to the ground truth or the best relaying scheme (such that 0 stands for CF and 1 for DF) obtained by the first selection method (Section IV-A), where the data rates and primary degradation are computed given the true channels and predicted powers based on the imperfect CSI; and $\hat{y}_i \in [0, 1]$ is the probability of selecting DF computed by the DNN.

The architecture of the considered DNN for relaying selection, depicted in Figure 9, is similar to the previous DNNs for solving the power allocation problem.

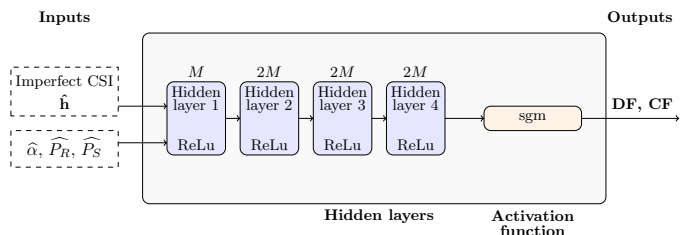


Figure 9: Proposed DNN architecture to choose among CF and DF with a fixed decision threshold at 0.5 (Extra-DNN).

The decision to use the same DNN architecture for an entirely different problem can be justified due to the similarities in data characteristics. Both problems involve imperfect CSI as inputs, indicating a resemblance in the underlying data structure. Moreover, the fully connected architecture is justified because of its generality and given that there is no a priori structural or temporal information within the inputs to be exploited via more specialized architectures such as convolutional or recurrent network. Therefore, it is intuitive to conclude that changing the DNN architecture would not yield significant benefits, given the similarities in data and the DNN's proven effectiveness in related problems. For the relaying scheme selection, we increase the number of neurons to $M = 256$ (instead of value $M = 128$ used for the power allocation prediction) as we empirically found that this value achieves good performance. Also, the final layer consists here in a sigmoid activation function outputting the

probability \hat{y}_i of selecting DF; the later is then compared to a threshold, set either to 0.5 or to a cognitive radio-tailored one allowing to minimize the average primary degradation when in outage Δ_{out} , to decide whether CF or DF should be selected (Figure 10).

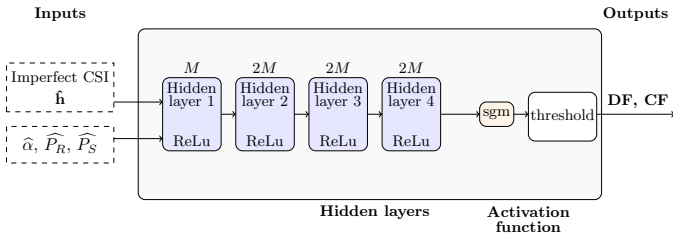


Figure 10: Proposed DNN architecture to choose among CF and DF with a finely tuned threshold (Extra-DNN-S).

The threshold is essential to take into account because its choice can significantly impact the performance of the supervised DNN model. This cognitive radio-tailored threshold is obtained by exhaustive search for each value of the channel estimation quality. In Table I, we present the best obtained thresholds used for Extra DNN-S as a function of SNR. If the predicted output value of the supervised DNN is below the threshold, the selected relaying scheme is CF; otherwise, the selected relaying scheme is DF.

Table I: Best threshold as a function of SNR

SNR (dB)	-10	-5	0	5	10	15	20
threshold	0.09	0.01	0.01	0.02	0.04	0.06	0.10

C. Numerical results

Before we present the experimental result of our proposed relay selection scheme, we describe the dataset construction and the DNN training (for the second method).

a) Dataset: The channel gains follow the same common fading and pathloss model as in Section III-D and are impaired by channel estimation errors, as in Section III-C. The training set contains 10^7 samples of perfect and imperfect channel estimation \mathbf{h}_ℓ and $\hat{\mathbf{h}}_\ell$, the associated optimal powers obtained via the self-supervised DNN described in Section III-C as well as the corresponding best relaying scheme obtained via the first selection method (where the data rates and primary degradation are computed with the true channels and power predicted with imperfect CSI).

The validation set is obtained as an excluded (20%) subset of the training set and our test set contains 2×10^6 samples of imperfect channel estimation with the corresponding optimal powers and the best relaying scheme as ground truth, enabling to assess the performance of our proposed approach.

To simplify the presentation of our numerical simulations, we will use the following terminology: “Two-DNN” refers to the benchmark selection method where imperfect CSI is used both to predict the transmission parameters (i.e., power allocation policies and relay selection scheme) and to compute the achievable rates and primary degradation used in our first selection scheme. “Extra-DNN” refers to the second relaying

scheme selection method, where the threshold is set to 0.5, and “Extra-DNN-S” refers to the second relaying selection method with a different and tailored threshold to the cognitive radio network under study.

b) DNN training: In the training phase, the optimal relaying scheme computed via the Two-DNN method (where the rates and primary degradation are computed using the true channels but with powers predicted using the imperfect channels) is fed to our loss function in (5), whereas the imperfect channel estimations and the corresponding optimal powers under both DF and CF, obtained with the DNN methods of Section III are given as the input of our additional DNN. Note that the training process is restarted for each value of the considered SNR of the CSI estimator. Here, the patience parameter is set to 10 epochs for both DF and CF to avoid any overfitting effect.

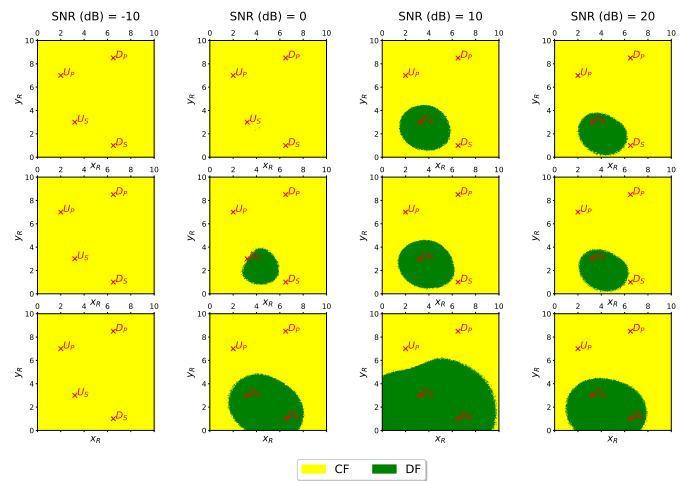


Figure 11: The selected relaying scheme between CF and DF. Top figures: Two DNN, middle: Extra-DNN, bottom: Extra DNN-S.

c) Numerical simulations: Figure 11 shows the selected relaying scheme as a function of the relay position for the methods: Two-DNN, Extra-DNN and Extra-DNN-S, and assuming different levels of CSI estimation quality. Here, we assume that the position of the primary and secondary users and destinations are fixed, whereas the relay can be positioned anywhere.

First, we can note that, regardless of the quality of the CSI estimation, CF is selected more often than DF under all approaches, which is to be expected since DF is limited by the fact that the relay needs to be able to decode the message from the secondary transmitter. Furthermore, as also expected from a cooperative communications point of view, DF is more efficient when the relay is close to the secondary transmitter, which can be observed for a CSI estimation quality between 0 – 20 dB under the fixed-threshold Extra-DNN and the Two-DNN methods.

Remarkably, for the Extra-DNN-S method, the set of relay positions where DF outperforms CF also contains positions where the relay is close to the secondary destination, for which the achievable data rate under DF is not expected to be large. The intuition is that our relay selection methods prioritizes the primary degradation over the achievable secondary rate.

For these relay positions, CF achieves higher rates than DF by also consuming more transmit power, leading hence to larger primary degradation. We can observe that as the channel quality increases (10–20) dB, the region in which DF relaying scheme is selected first expands (10 dB), but then contracts again when SNR = 20 dB. This phenomenon can be justified by the fact that, with an SNR of the channels estimation of 10 dB, the DNN chooses the relaying scheme that maximizes throughput and exhibits less sensitivity to imperfect CSI, favoring DF as can be confirmed from Figure 5 and Figure 7. Conversely, at higher SNR levels (20 dB), CF relaying displays lower sensitivity to imperfect CSI and outperforms DF in terms of throughput in more regions (Figure 5 and Figure 7), resulting in a preference for CF relaying in more regions.

Finally, under all approaches and irrespective from the position of the relay, CF is almost always chosen in very poor CSI estimation conditions –10 dB. DF seems indeed to be more sensitive to imperfect CSI, since the relay needs to correctly decode the secondary message; while it only quantizes the received signal under CF relaying.

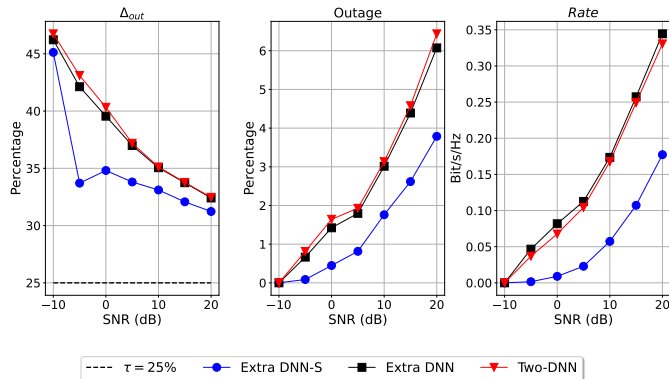


Figure 12: Average degradation when in outage, outage and secondary rate as functions of SNR over the test set.

In Figure 12, we compare the three methods: Two-DNN, Extra-DNN and Extra-DNN-S, in terms of primary rate degradation when in outage Δ_{out} , percentage of outage and secondary rate as functions of the CSI estimation SNR. First, we notice that Two-DNN and Extra-DNN achieve more or less the same performance, meaning that there was little additional information to be learned between the channel gains and the best relaying scheme. This highlights the strength of our proposed DNN-based power allocation policy for a fixed relaying scheme. This can also be explained by fact that each of the two relaying schemes (CF and DF) perform best for disjoint relay positions.

Second, by tuning the threshold which minimizes the primary rate degradation when in outage, as performed for Extra-DNN-S, significantly increases the performance in terms of primary degradation: the number of outage events is divided by a factor of almost 2 for all values of SNR $\in [-10, 20]$ dB, whereas the primary degradation when in outage is decreased by up to 8% especially under poor channel estimation conditions. Of course, the prioritized primary protection comes at the cost of secondary rate, which is decreased as shown.

At last, using an additional DNN enables us to generalize over which criterion the relaying scheme should be selected. Indeed, here, the relay scheme selection was decided based on the minimization of the primary rate degradation when in outage. One could consider any tradeoff weighting between the secondary rate and primary protection instead, which is not feasible under the two DNN-based method.

V. GENERALIZED DNN SOLUTION

While in the previous sections the maximum allowed primary rate degradation τ , as well as the power budget within the secondary network \overline{P}_R and \overline{P}_S were fixed, we propose here to generalize our self-supervised DNN approach in terms of the system parameters: τ , \overline{P}_R , and \overline{P}_S assuming that they lie within specified ranges.

A. Proposed Generalized DNN Solution

Although the system parameters are no longer fixed, the loss function to be minimized by the self-supervised DNN remains essentially the same as in Section III. The main difference with the case of fixed parameters is that the values of τ , \overline{P}_R , \overline{P}_S have to be provided as inputs of both the self-supervised DNN and the loss function.

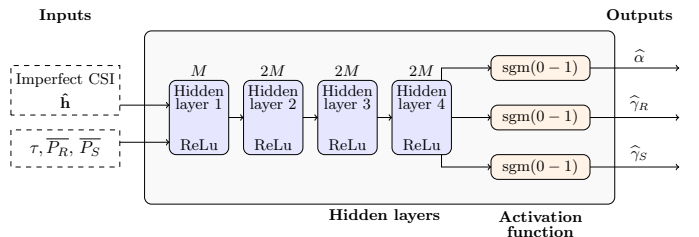


Figure 13: DNN^\dagger : Proposed DNN-based generalization over both the maximum allowed primary rate degradation and the power budgets.

Figure 13 presents the architecture of our proposed self-supervised DNN, thereafter denoted by DNN^\dagger , able to generalize jointly over all τ and the power budgets. This architecture is very similar to the one in Section III when τ and the power budgets were fixed. The main differences are the following: i) τ , \overline{P}_S and \overline{P}_R are provided as *inputs* of the DNN^\dagger ; ii) DNN^\dagger has to *output* the fractions $\hat{\gamma}_R \in [0, 1]$ and $\hat{\gamma}_S \in [0, 1]$ of the relay and secondary power to be consumed, instead of directly the estimated powers \hat{P}_R and \hat{P}_S computed as $\hat{P}_i = \overline{P}_i \hat{\gamma}_i, i \in \{R, S\}$. Aside from these modifications, the remaining inner self-supervised DNN architecture, i.e., the number of layers and the number of neurons per layer, remains the same as in Section III.

This new architecture can also be used to study the partial generalization over either τ for fixed power budgets, thereafter denoted by DNN_τ , or over the power budgets for a fixed τ , denoted by DNN_P . In these architectures, the fixed parameters values are no longer provided as inputs of the DNN, i.e., DNN_τ has only two inputs ($\hat{\mathbf{h}}, \tau$) and DNN_P three inputs ($\hat{\mathbf{h}}, \overline{P}_R, \overline{P}_S$).

B. Computational costs analysis

In this subsection, we compare the three approaches (DNN_τ , DNN_P , and DNN^\dagger) in terms of number of trainable parameters and FLOPs (Floating Point Operations). For the test phase, the three DNNs differences in computational cost are minimal because they all share a very similar architecture and only differ in the first layer of the DNN. Therefore, during the test phase, we only compare the memory cost.

For the training phase, the trainable parameters refer to the learnable parameters: weights and biases, within a neural network model that are updated during the training process. These parameters are the variables that the model learns from the training data to make predictions or perform specific tasks. It is important to note that the number of trainable parameters is not the same for the DNN_τ , DNN_P , and DNN^\dagger , because for DNN_τ we have two inputs, namely $\hat{\mathbf{h}}$ and τ , and for DNN_P we have three inputs, namely $\hat{\mathbf{h}}$, $\overline{P_R}$ and $\overline{P_S}$, and for DNN^\dagger we have four inputs, namely $\hat{\mathbf{h}}$, τ , $\overline{P_R}$ and $\overline{P_S}$.

FLOPs specifically refer to the number of floating-point operations, which include addition, subtraction, multiplication, and division operations. The number of FLOPs is commonly used to measure the computational complexity or cost of a model. The higher the number of FLOPs a model requires, the more computationally intensive it is.

Table II: FLOPs and Parameters as functions of DNNs for CF

DNNs	DNN_τ	DNN_P	DNN^\dagger
FLOPs	331,908	332,162	332,418
Parameters	166,402	166,530	166,658

Table III: FLOPs and Parameters as functions of DNNs for DF

DNNs	DNN_τ	DNN_P	DNN^\dagger
FLOPs	332,421	332,675	332,931
Parameters	166,659	166,787	166,915

In Table II and Table III, we present the total number of FLOPs and trainable parameters under CF and DF relaying using our three different DNNs. In the training phase, it is recommended to use DNN^\dagger due to its efficiency, rather than DNN_τ , and DNN_P . This choice is advantageous for several reasons. In Table II, when comparing the number of trainable parameters and the number of FLOPs, we note that regardless of the used DNN architecture, whether it involves two or multiple inputs, it is primarily the first layer that costs slightly more per inputs. This is why, in terms of the number of FLOPs and number of parameters, we do not have a significant difference that would make one DNN excessively more complex or simpler than the other.

In the test phase, the memory cost is not the same for the three DNNs, because if we want to generalize over 10 values of τ and 10 values of power budgets exploiting both DNN_τ and DNN_P , we would need to train and store 100 DNNs, which is expensive in terms of both computation and storage. In contrast, for DNN^\dagger , we would need to train and store it only once, and it can generalize for any given values of τ and power budgets. Furthermore, we achieve almost the same communication performance (in terms of achievable rate,

outage, etc.) with DNN^\dagger , than with DNN_τ and DNN_P without increasing the size of the dataset.

C. Numerical results

a) *Datasets*: As in the previous sections, we assume that only imperfect CSI samples are available in the test set, whereas pairs of both perfect and imperfect CSI are available in the training and validation sets. In order to ease the presentation, we will separate the three datasets used for the self-supervised DNN able to generalize over τ , over the power budget and over all system parameters respectively.

i) The training set assessing the generalization over the primary degradation τ is composed of 10^6 samples of $\{\mathbf{h}_\ell, \hat{\mathbf{h}}_\ell, \tau_\ell\}_\ell$, where each of the realization τ_ℓ is within the range $\tau_\ell \in [0.1, 0.5]$. The corresponding test set contains 2×10^5 samples of $\{\mathbf{h}_\ell, \tau_\ell\}_\ell$.

ii) The training set assessing the generalization over the power budget is composed of 2×10^6 samples of $\{\mathbf{h}_\ell, \hat{\mathbf{h}}_\ell, \overline{P_{S,\ell}}, \overline{P_{R,\ell}}\}_\ell$, where each of the realization $\overline{P_{S,\ell}}, \overline{P_{R,\ell}}$ is within the range $\overline{P_{S,\ell}}, \overline{P_{R,\ell}} \in [1, 10] \times [1, 10]$, and that the powers are interdependent, such as $\overline{P_{S,\ell}} = \overline{P_{R,\ell}}$. The corresponding test set contains 4×10^5 samples of $\{\mathbf{h}_\ell, \overline{P_{S,\ell}}, \overline{P_{R,\ell}}\}_\ell$.

iii) The training set assessing the generalization over the three system parameters is composed of 2×10^6 samples of $\{\mathbf{h}_\ell, \hat{\mathbf{h}}_\ell, \tau_\ell, \overline{P_{S,\ell}}, \overline{P_{R,\ell}}\}_\ell$, where each of the realization τ_ℓ is within the range $\tau_\ell \in [0.1, 0.5]$ and $\overline{P_{S,\ell}}, \overline{P_{R,\ell}}$ is within the range $\overline{P_{S,\ell}}, \overline{P_{R,\ell}} \in [1, 10] \times [1, 10]$, with $\overline{P_{S,\ell}} = \overline{P_{R,\ell}}$. The corresponding test set contains 4×10^5 samples of $\{\hat{\mathbf{h}}_\ell, \tau_\ell, \overline{P_{S,\ell}}, \overline{P_{R,\ell}}\}_\ell$.

In all cases, the validation set is obtained as an excluded (20%) subset of the training set.

b) *DNN training*: As in the previous sections, the self-supervised DNNs are provided $\{\mathbf{h}_\ell, \tau_\ell\}$ or $\{\hat{\mathbf{h}}_\ell, \overline{P_{S,\ell}}, \overline{P_{R,\ell}}\}$, or $\{\hat{\mathbf{h}}_\ell, \tau_\ell, \overline{P_{S,\ell}}, \overline{P_{R,\ell}}\}$ as inputs, whereas the perfect CSI \mathbf{h}_ℓ and the values of τ or $\overline{P_R}, \overline{P_S}$ are only fed to the loss function as $\{\mathbf{h}_\ell, \tau_\ell\}$ or $\{\mathbf{h}_\ell, \overline{P_{S,\ell}}, \overline{P_{R,\ell}}\}$, or $\{\mathbf{h}_\ell, \tau_\ell, \overline{P_{S,\ell}}, \overline{P_{R,\ell}}\}$. The training process is restarted for each value of the considered channel estimation SNR, and the patience parameter is set to 10 epochs under both DF and CF to avoid any overfitting effects.

c) *Numerical simulations*: In the following, we only present the performance obtained with CF relaying because of space issues. Similar observations and conclusions carry over also under DF relaying.

To evaluate the ability of our proposed DNN^\dagger to generalize jointly over τ and the power budgets, we propose to consider two cases: either fixed power budgets and varying τ , or varying power budgets while keeping τ fixed. Indeed, interpreting the results while changing all parameters at once is challenging, as we cannot discern whether the DNN^\dagger is generalizing well on τ or the power budgets or both.

In Figure 14, we plot the outage, the average primary rate degradation (Δ_ℓ), the average and maximum primary rate degradation when in outage (Δ_{out} and Δ_{max} respectively) as well as the mean of the secondary rate and the mean plus and minus the standard deviation of the secondary rate, for different qualities of channel estimator $\text{SNR} \in [-10, 20]$

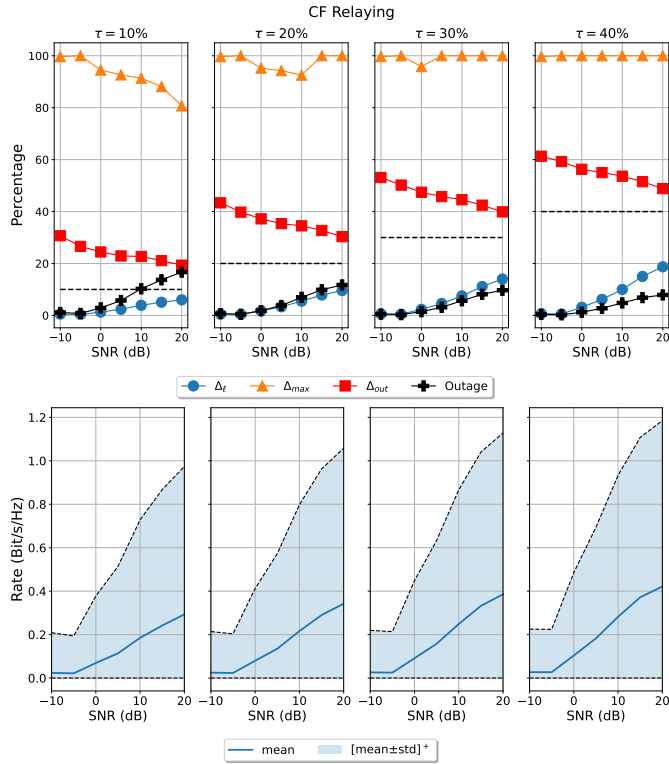


Figure 14: Joint generalization over the secondary power budgets and the maximum allowed primary degradation with DNN^\dagger and under CF relaying: impact of the maximum allowed primary degradation when $\bar{P}_R = \bar{P}_S = 10$ W.

dB with the DNN^\dagger and for CF relaying. These results were obtained for $\bar{P}_R = \bar{P}_S = 10$ W and $\tau \in \{0.1, 0.2, 0.3, 0.4\}$.

We can note that our proposed DNN^\dagger generalizes over different values of τ since the average primary degradation (Δ_ℓ) stays below the threshold τ , regardless of its value for fixed secondary power budget $\bar{P}_R = \bar{P}_S = 10$ W. As expected, the percentage of average primary rate degradation (Δ_ℓ) and the secondary rate increase with the value of τ , since the secondary network is allowed to transmit with higher levels of power. Nonetheless, even if the percentage of average primary degradation increases (while remaining below the threshold of τ), the average primary rate degradation when in outage remains close to the threshold of τ , especially for moderate to good channel estimations. These results are also very close to the ones obtained with DNN_τ , which only generalizes over the value of τ for fixed power budgets (omitted here because of space limitation), validating the ability of DNN^\dagger to generalize over τ when fed with a fixed power budget value.

In Figure 15, we illustrate the same performance metrics as in Figure 14 for different qualities of channel estimator $\text{SNR} \in [-10, 20]$ dB for the DNN^\dagger by fixing $\tau = 25\%$. Note that similar conclusions carry over for the generalization over the power budgets varying within $\bar{P}_R = \bar{P}_S \in \{2.5, 5, 7.5, 10\}$ W. Here, even if the percentage of outage also increases for larger power budgets, as expected, the average primary degradation remains below the threshold of τ . Finally, the performance obtained by DNN_P that only generalizes over the power budgets and the one obtained by DNN^\dagger are very close, validating hence

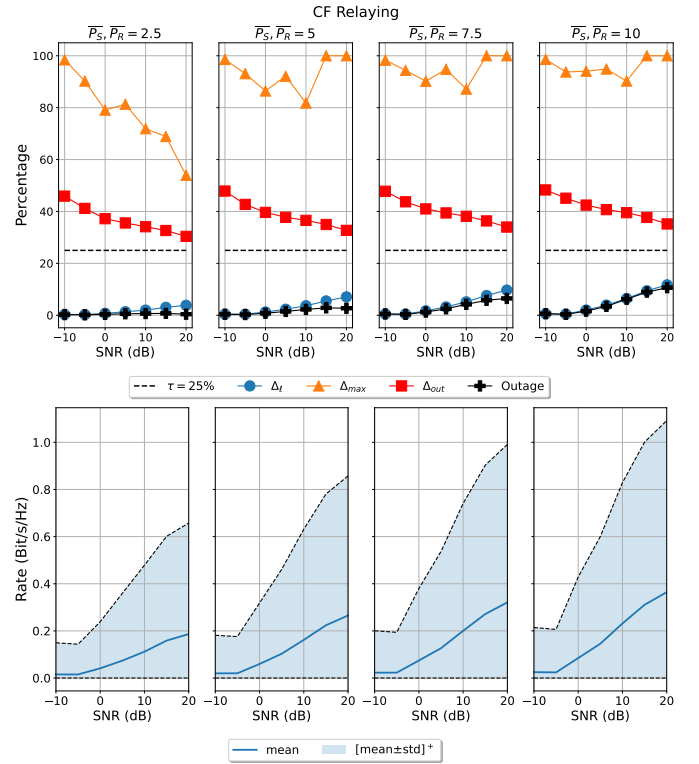


Figure 15: Joint generalization over the secondary power budget and the maximum allowed primary degradation with DNN^\dagger and under CF relaying: impact of secondary power budget when $\tau = 0.25$.

the ability of DNN^\dagger to generalize over the power budgets when fed with a fixed value of τ .

To sum up, we have shown that our self-supervised DNN-based power allocation policy under imperfect CSI in Section III can generalize well over various system parameters, by simply adding them as input features with little change in the architecture of the DNN and its training procedure (w.r.t. the custom loss function and datasets).

VI. CONCLUSIONS AND PERSPECTIVES

In this paper, we proposed a novel self-supervised DNN-based power allocation policy maximizing the opportunistic rate of a relay-aided (performing either DF or CF relaying) cognitive radio system protected by a primary QoS constraint and limited by individual power budgets. We first show the robustness of our approach to imperfect CSI. We then extend it to also select the best relaying scheme that tradeoffs opportunistic rate vs. primary protection. Finally, we show how our approach can be generalized across different system parameters, i.e., the primary protection parameter and the power budgets. Interesting future work includes the investigation of the secondary outage probability in the imperfect CSI case and the evaluation of proposed approach on more realistic data built with Sionna [49], an open-source GPU-accelerated link-level simulator exploiting Ray-tracing capabilities in wireless 5G/6G networks. Additionally, we aim to explore more complex multi-user settings and investigate few-shot learning to address settings with limited available training data.

REFERENCES

- [1] M. Z. Chowdhury, M. Shahjalal, S. Ahmed, and Y. M. Jang, "6G wireless communication systems: Applications, requirements, technologies, challenges, and research directions," *IEEE Open J. Commun. Soc.*, vol. 1, pp. 957–975, 2020.
- [2] F. Tariq, M. R. A. Khandaker, K.-K. Wong, M. A. Imran, M. Bennis, and M. Debbah, "A speculative study on 6G," *IEEE Wireless Commun.*, vol. 27, no. 4, pp. 118–125, 2020.
- [3] W. Saad, M. Bennis, and M. Chen, "A vision of 6G wireless systems: Applications, trends, technologies, and open research problems," *IEEE Netw.*, vol. 34, no. 3, pp. 134–142, 2020.
- [4] S. Buzzi, C.-L. I. T. E. Klein, H. V. Poor, C. Yang, and A. Zappone, "A survey of energy-efficient techniques for 5G networks and challenges ahead," *IEEE J. Sel. Areas Commun.*, vol. 34, no. 4, pp. 697–709, 2016.
- [5] S. K. Nobar, M. H. Ahmed, Y. Morgan, and S. A. Mahmoud, "Resource allocation in cognitive radio-enabled UAV communication," *IEEE Trans. on Cogn. Commun. Netw.*, vol. 8, no. 1, pp. 296–310, 2022.
- [6] S. Devipriya, J. M. Leo Manickam, and K. Jasmine Mystica, "A Deep-learning based approach to resource allocation in NOMA based cognitive radio network with heterogeneous IoT users," in *IEEE ICDCECE*, 2022, pp. 1–6.
- [7] S. Dhanasekaran and C. M., "Performance analysis of NOMA in full-duplex cooperative spectrum sharing systems," *IEEE Trans. Veh. Technol.*, vol. 71, no. 8, pp. 9095–9100, 2022.
- [8] G. Zhang, Y. Wang, Y. Wang, H. Ding, W. Wang, and Z. Bai, "Power allocation for multi-relay af cooperative system with maximum system capacity," in *ICACT*, 2020, pp. 109–113.
- [9] A. Savard and E. V. Belmega, "Optimal power allocation policies in multi-hop cognitive radio networks," in *IEEE PIMRC*, 2020, pp. 1–6.
- [10] E. C. Van Der Meulen, "Three-terminal communication channels," *Adv. Appl. Probab.*, vol. 3, no. 1, p. 120–154, 1971.
- [11] T. Cover and A. Gamal, "Capacity theorems for the relay channel," *IEEE Trans. Inf. Theory*, vol. 25, no. 5, pp. 572–584, 1979.
- [12] L. Zhang, Y.-C. Liang, and D. Niyato, "6G visions: Mobile ultra-broadband, super internet-of-things, and artificial intelligence," *China Commun.*, vol. 16, no. 8, pp. 1–14, 2019.
- [13] C.-X. Wang, M. D. Renzo, S. Stanczak, S. Wang, and E. G. Larsson, "Artificial intelligence enabled wireless networking for 5G and beyond: Recent advances and future challenges," *IEEE Wireless Commun.*, vol. 27, no. 1, pp. 16–23, 2020.
- [14] F. Liang, C. Shen, W. Yu, and F. Wu, "Power control for interference management via ensembling deep neural networks," in *IEEE/CIC ICC*, 2019, pp. 237–242.
- [15] W. Lee, "Resource allocation for multi-channel underlay cognitive radio network based on deep neural network," *IEEE Commun. Lett.*, vol. 22, no. 9, pp. 1942–1945, 2018.
- [16] Y. Benatia, R. Negrel, A. Savard, and E. V. Belmega, "Robustness to imperfect CSI of power allocation policies in cognitive relay networks," in *IEEE SPAWC*, 2022, pp. 1–5.
- [17] A. Savard and E. V. Belmega, "Full-duplex relaying for opportunistic spectrum access under an overall power constraint," *IEEE Access*, vol. 8, pp. 168 262–168 272, 2020.
- [18] Y. Benatia, A. Savard, R. Negrel, and E. V. Belmega, "Unsupervised deep learning to solve power allocation problems in cognitive relay networks," in *IEEE ICC Workshops*, 2022, pp. 331–336.
- [19] Q. Shi, M. Razaviyayn, Z.-Q. Luo, and C. He, "An iteratively weighted MMSE approach to distributed sum-utility maximization for a MIMO interfering broadcast channel," *IEEE Trans. Signal Process.*, vol. 59, no. 9, pp. 4331–4340, 2011.
- [20] Q. Qi, A. Minturn, and Y. Yang, "An efficient water-filling algorithm for power allocation in OFDM-based cognitive radio systems," in *IEEE ICSSAI*, 2012, pp. 2069–2073.
- [21] W. Lee and R. Schober, "Deep learning-based resource allocation for device-to-device communication," *IEEE Trans. Wireless Commun.*, vol. 21, no. 7, pp. 5235–5250, 2022.
- [22] W. Lee and K. Lee, "Robust transmit power control with imperfect CSI using a deep neural network," *IEEE Trans. Veh. Technol.*, vol. 70, no. 11, pp. 12 266–12 271, 2021.
- [23] A. B. Adam, L. Lei, S. Chatzinotas, and N. U. R. Junejo, "Deep convolutional self-attention network for energy-efficient power control in NOMA networks," *IEEE Trans. Veh. Technol.*, 2022.
- [24] Y. Zhao, I. G. Niemegeers, and S. M. H. De Groot, "Dynamic power allocation for cell-free massive MIMO: Deep reinforcement learning methods," *IEEE Access*, vol. 9, pp. 102 953–102 965, 2021.
- [25] D. Kim, H. Jung, and I.-H. Lee, "User selection and power allocation scheme with SINR-based deep learning for downlink NOMA," *IEEE Trans. Veh. Technol.*, 2023.
- [26] —, "Deep learning-based power control scheme with partial channel information in overlay device-to-device communication systems," *IEEE Access*, vol. 9, pp. 122 125–122 137, 2021.
- [27] H. Sun, X. Chen, Q. Shi, M. Hong, X. Fu, and N. D. Sidiropoulos, "Learning to optimize: Training deep neural networks for wireless resource management," in *IEEE SPAWC*. IEEE, 2017, pp. 1–6.
- [28] V. Sze, Y.-H. Chen, T.-J. Yang, and J. S. Emer, "Efficient processing of deep neural networks: A tutorial and survey," *Proc. IEEE*, vol. 105, no. 12, pp. 2295–2329, 2017.
- [29] F. Hussain, S. A. Hassan, R. Hussain, and E. Hossain, "Machine learning for resource management in cellular and IoT networks: Potentials, current solutions, and open challenges," *IEEE Commun. Surveys Tuts.*, vol. 22, no. 2, pp. 1251–1275, 2020.
- [30] Z. Shao, J. Yang, C. Shen, and S. Ren, "Learning for robust combinatorial optimization: Algorithm and application," in *IEEE INFOCOM*, 2022, pp. 930–939.
- [31] A. Zappone, M. Di Renzo, and M. Debbah, "Wireless networks design in the era of deep learning: Model-based, AI-based, or both?" *IEEE Trans. Commun.*, vol. 67, no. 10, pp. 7331–7376, 2019.
- [32] K. Lee, J.-R. Lee, and H.-H. Choi, "Learning-based joint optimization of transmit power and harvesting time in wireless-powered networks with co-channel interference," *IEEE Trans. Veh. Technol.*, vol. 69, no. 3, pp. 3500–3504, 2020.
- [33] W. Lee and K. Lee, "Deep learning-aided distributed transmit power control for underlay cognitive radio network," *IEEE Trans. Veh. Technol.*, vol. 70, no. 4, pp. 3990–3994, 2021.
- [34] W. Lee and B. C. Chung, "Ensemble deep learning based resource allocation for multi-channel underlay cognitive radio system," *ICT Express*, 2022.
- [35] M. Lu, B. Zhou, Z. Bu, and Y. Zhao, "A learning approach towards power control in full-duplex underlay cognitive radio networks," in *IEEE WCNC*, 2022, pp. 2017–2022.
- [36] S. S. Ikki and M. H. Ahmed, "Performance analysis of adaptive decode-and-forward cooperative diversity networks with best-relay selection," *IEEE Trans. Commun.*, vol. 58, no. 1, pp. 68–72, 2010.
- [37] A. Abdelreheem, O. A. Omer, H. Esmail, and U. S. Mohamed, "Deep learning-based relay selection in D2D millimeter wave communications," in *IEEE ICCIS*, 2019, pp. 1–5.
- [38] S. Aldossari and K.-C. Chen, "Relay selection for 5G new radio via artificial neural networks," in *IEEE WPMC*, 2019, pp. 1–5.
- [39] T.-V. Nguyen, T. Huynh-The, and B. An, "A deep CNN-based relay selection in EH full-duplex IoT networks with short-packet communications," in *IEEE ICC*, 2021, pp. 1–6.
- [40] T. T. Duy and H. Y. Kong, "Performance analysis of mixed amplify-and-forward and decode-and-forward protocol in underlay cognitive networks," *China Commun.*, vol. 13, no. 3, pp. 115–126, 2016.
- [41] D. P. Setiawan and H.-A. Zhao, "Performance analysis of hybrid AF and DF protocol for relay networks," in *IEEE ICCREC*, 2017, pp. 207–211.
- [42] X. Zong, X. Zhu, A. Zhu, and J. O. Byrne, "Optimization and transmit power control based on deep learning with inaccurate channel information in underlay cognitive radio network," in *J. Phys. Conf. Ser.*, vol. 1746, no. 1. IOP Publishing, 2021, p. 012090.
- [43] A. Savard and E. V. Belmega, "Optimal power allocation in a relay-aided cognitive network," in *EAI ValueTools*, 2019, pp. 15–22.
- [44] V. Rizzello and W. Utschick, "Learning the CSI denoising and feedback without supervision," in *IEEE SPAWC*, 2021, pp. 16–20.
- [45] X. Song, L. Dong, J. Wang, L. Qin, and X. Han, "Energy efficient power allocation for downlink NOMA heterogeneous networks with imperfect CSI," *IEEE Access*, vol. 7, pp. 39 329–39 340, 2019.
- [46] B. I. Justusson, *Median Filtering: Statistical Properties*. Berlin, Heidelberg: Springer Berlin Heidelberg, 1981, pp. 161–196. [Online]. Available: <https://doi.org/10.1007/BFb0057597>
- [47] T. Hastie, R. Tibshirani, J. H. Friedman, and J. H. Friedman, *The elements of statistical learning: data mining, inference, and prediction*. Springer, 2009, vol. 2.
- [48] S. Shalev-Shwartz and S. Ben-David, *Understanding machine learning: From theory to algorithms*. Cambridge university press, 2014.
- [49] J. Hoydis, S. Cammerer, F. A. Aoudia, A. Vem, N. Binder, G. Marcus, and A. Keller, "Sionna: An open-source library for next-generation physical layer research," *arXiv preprint arXiv:2203.11854*, 2022.